Z'-induced Invisible Right-handed Sneutrino Decays at the LHC

W. ABDALLAH

Center for Fundamental Physics
Zewail City of Science and Technology

This work in collaboration with J. Fiaschi, S. Khalil and S. Moretti

Phys. Rev. D **92**, 055029 (2015) [arXiv:1504.01761 [hep-ph]]

Outline

1 Motivation

Outline

1 Motivation

2 Analysis and Simulation

Outline

1 Motivation

2 Analysis and Simulation

3 Summary

Outline

1 Motivation

2 Analysis and Simulation

3 Summary

4 References

Outline

1 Motivation

2 Analysis and Simulation

3 Summary

4 References

- The advantage of the signal is that the final state objects carry a very large (transverse) missing energy, since the Z' is naturally massive and constrained by direct searches to be at least in the TeV scale region.
- Under these conditions the efficiency in accessing the invisible final state and rejecting the SM background is very high.
- Another special feature of this invisible BLSSM signal is its composition, which is often dominated by RH sneutrino decays.
- Sensitivity of the CERN machine can therefore help disentangling the BLSSM from more popular SUSY models.

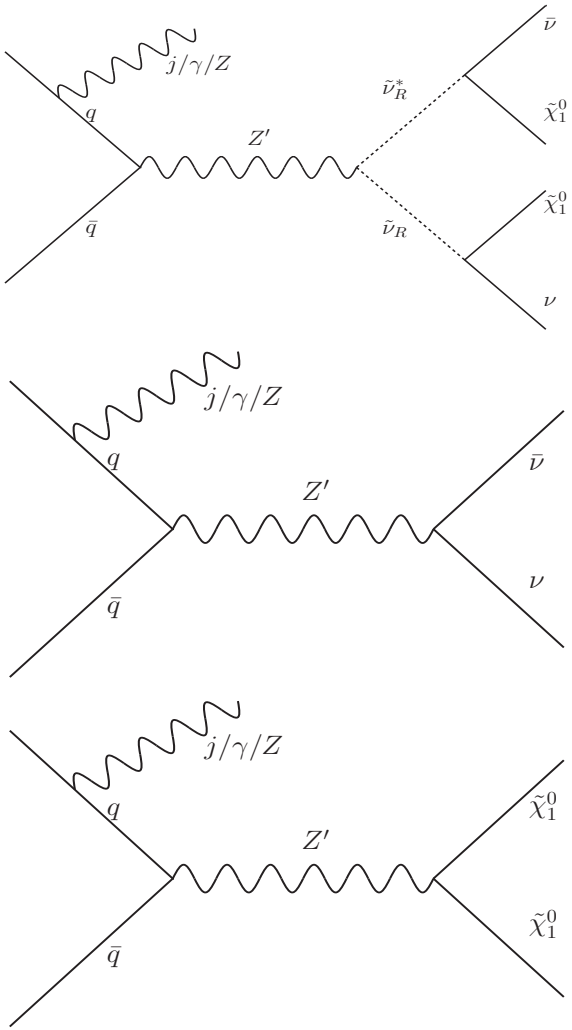

- The advantage of the signal is that the final state objects carry a very large (transverse) missing energy, since the Z' is naturally massive and constrained by direct searches to be at least in the TeV scale region.
- Under these conditions the efficiency in accessing the invisible final state and rejecting the SM background is very high.
- Another special feature of this invisible BLSSM signal is its composition, which is often dominated by RH sneutrino decays.
- Sensitivity of the CERN machine can therefore help disentangling the BLSSM from more popular SUSY models.

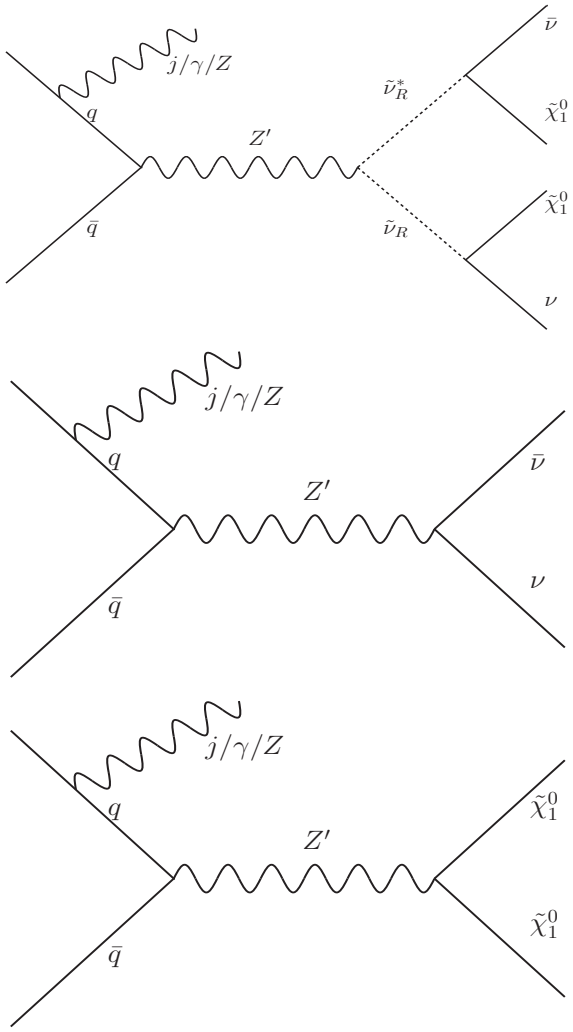

BLSSM $\tilde{\nu}_R$

Outline

1 Motivation

2 Analysis and Simulation

3 Summary

4 References

- The matrix-elements for the parton level signals and backgrounds were calculated by using MadGraph5. PYTHIA have been used for showering and hadronisation, whereas we have performed the fast detector simulations with PGS4.

- The matrix-elements for the parton level signals and backgrounds were calculated by using MadGraph5. PYTHIA have been used for showering and hadronisation, whereas we have performed the fast detector simulations with PGS4.
- For MC efficiency and in order to obtain reasonable statistics, we have applied a parton level (generation) cut of $p_T(j_1) > 120$ GeV for all signals and backgrounds.

- The matrix-elements for the parton level signals and backgrounds were calculated by using MadGraph5. PYTHIA have been used for showering and hadronisation, whereas we have performed the fast detector simulations with PGS4.
- For MC efficiency and in order to obtain reasonable statistics, we have applied a parton level (generation) cut of $p_T(j_1) > 120$ GeV for all signals and backgrounds.
- According to the estimation of the QCD background in the SUSY mono-jets analysis, the multi-jet background can be reduced to a negligible level by requiring a large $\not{E}_T$ cut, so we have applied another parton level cut of $\not{E}_T > 100$ GeV for both signals and backgrounds.

- The dominant SM backgrounds:

- The dominant SM backgrounds:
  1. the irreducible background $pp \to Z(\to \nu\bar{\nu}) + j$, which is the main one because it has the same topology as our signals;

- The dominant SM backgrounds:
  1. the irreducible background $pp \to Z(\to \nu\bar{\nu}) + j$, which is the main one because it has the same topology as our signals;
  2. $pp \to W(\to \ell\nu) + j$ $(\ell = e, \mu)$, it fakes the signal only when the charged lepton is outside the acceptance of the detector or close to the jet;

- The dominant SM backgrounds:
  1. the irreducible background $pp \to Z(\to \nu\bar{\nu}) + j$, which is the main one because it has the same topology as our signals;
  2. $pp \to W(\to \ell\nu) + j$ $(\ell = e, \mu)$, it fakes the signal only when the charged lepton is outside the acceptance of the detector or close to the jet;
  3. $pp \to W(\to \tau\nu) + j$, it may fake the signal since a secondary jet from hadronic tau decays tend to localize on the side opposite to $\not{E}_T$;

- The dominant SM backgrounds:
  1. the irreducible background $pp \to Z(\to \nu\bar{\nu}) + j$, which is the main one because it has the same topology as our signals;
  2. $pp \to W(\to \ell\nu) + j$ $(\ell = e, \mu)$, it fakes the signal only when the charged lepton is outside the acceptance of the detector or close to the jet;
  3. $pp \to W(\to \tau\nu) + j$, it may fake the signal since a secondary jet from hadronic tau decays tend to localize on the side opposite to $\not{E}_T$;
  4. $pp \to t\bar{t}$, it may resemble the signal but also contains extra jets and leptons, which allow one to highly suppress it by applying b-jet and lepton vetoes;

- The dominant SM backgrounds:
  1. the irreducible background $pp \to Z(\to \nu\bar{\nu}) + j$, which is the main one because it has the same topology as our signals;
  2. $pp \to W(\to \ell\nu) + j$ $(\ell = e, \mu)$, it fakes the signal only when the charged lepton is outside the acceptance of the detector or close to the jet;
  3. $pp \to W(\to \tau\nu) + j$, it may fake the signal since a secondary jet from hadronic tau decays tend to localize on the side opposite to $\not{E}_T$;
  4. $pp \to t\bar{t}$, it may resemble the signal but also contains extra jets and leptons, which allow one to highly suppress it by applying b-jet and lepton vetoes;
  5. the di-boson background $pp \to ZZ(\to 2\nu 2\bar{\nu}) + j$, which is generically suppressed due to its small cross section at production level but topologically mimic our signals rather well.

- As explained, owing to the large mass of the Z', we can in the end afford a rather stiff cut in $\not{E}_T$ in order to enhance our signals. This is done by setting $\not{E}_T > 500$ GeV.

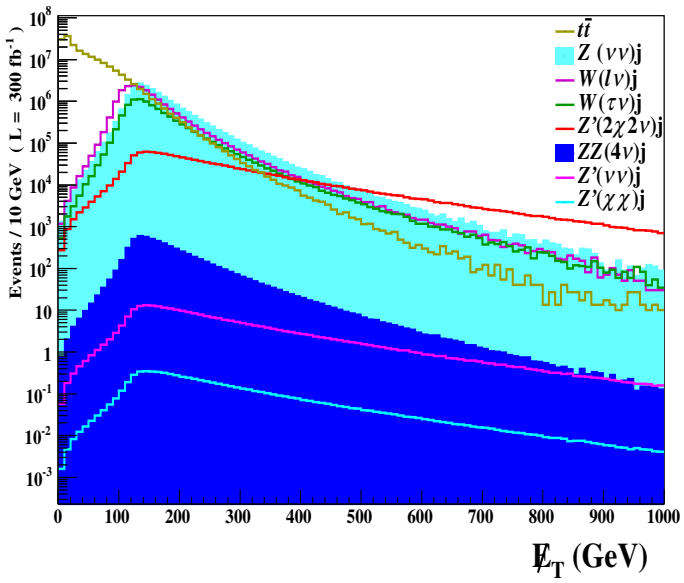

- As explained, owing to the large mass of the Z', we can in the end afford a rather stiff cut in $\not{E}_T$ in order to enhance our signals. This is done by setting $\not{E}_T > 500$ GeV.

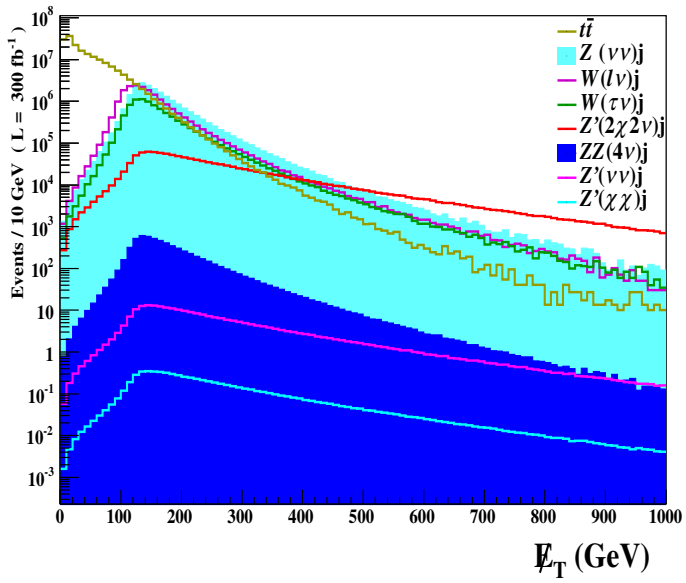

- This enhancement is also supplemented by requiring $p_T(j_1) > 500$ GeV as the signals have harder $p_T(j_1)$ spectra than the backgrounds.

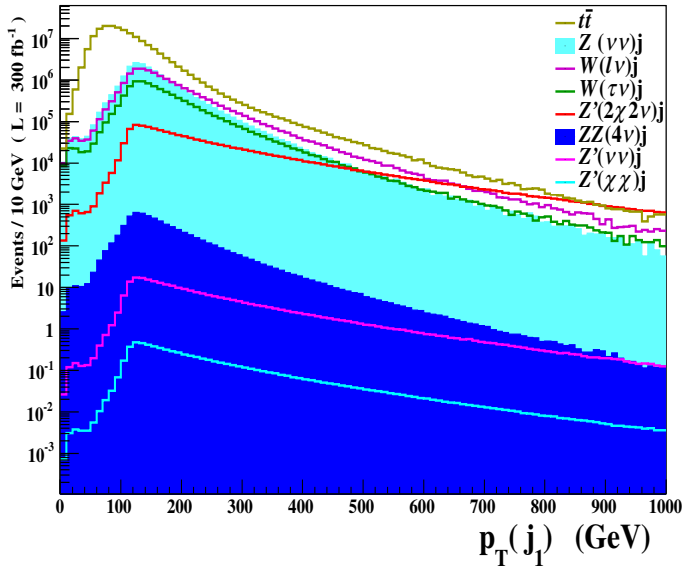

		Backgrounds					Signals		
Process		$Z(\nu\bar{\nu})j$	$W(l\nu_l)j$	$W(\tau\nu_\tau)j$	$t\bar{t}$	ZZj	$Z'(2\tilde{\chi}\,2\nu)j$	$Z'(\nu\bar{\nu})j$	$Z'(\tilde{\chi}\tilde{\chi})j$
Before cuts		21573000	19248000	9390000	179058000	6621	1334400	278	7.54
Cut	(1)	16823567 ± 1924	15817945 ± 1678	7719914 ± 1171	151390826 ± 4836	5732 ± 28	1219314 ± 324	255 ± 4.68	6.895 ± 0.77
	(2)	65275 ± 255	135191 ± 366	65423 ± 254	298430 ± 545	73 ± 8.5	130636 ± 343	27 ± 4.95	0.741 ± 0.82
	(3)	45530 ± 213	32569 ± 180	27102 ± 164	6836.8 ± 82.7	55.6 ± 7.43	118456 ± 328	25 ± 4.74	0.672 ± 0.78
	(4)	14283 ± 119	10566 ± 102	8668.5 ± 93.1	2808 ± 53	16.5 ± 4.06	35424 ± 185	7.4 ± 2.68	0.201 ± 0.44
	(5)	10831 ± 104	7395.3 ± 86	6088.7 ± 78	881.7 ± 29.7	12.2 ± 3.49	23330 ± 151	4.9 ± 2.18	0.132 ± 0.36
	(6)	8992.5 ± 94.8	6007.4 ± 77.5	4699.9 ± 68.5	379.8 ± 19.5	9.79 ± 3.13	18806 ± 136	3.9 ± 1.96	0.107 ± 0.33
	(7)	8969.8 ± 94.7	3343.1 ± 57.8	3929 ± 62.7	257.7 ± 16.1	9.78 ± 3.12	18786 ± 136	3.9 ± 1.96	0.107 ± 0.32
	(8)	8969.8 ± 94.7	871.2 ± 29.5	3207.4 ± 56.6	176.3 ± 13.3	9.77 ± 3.12	18782 ± 136	3.9 ± 1.96	0.107 ± 0.32
	(9)	8458.9 ± 92	790.2 ± 28.1	1378.8 ± 37.1	81.39 ± 9.02	9.21 ± 3.03	17878 ± 132	3.7 ± 1.92	0.102 ± 0.32
	(10)	8152.3 ± 90.3	769.9 ± 27.7	1334.4 ± 36.5	54.26 ± 7.37	8.8 ± 2.96	17357 ± 130	3.6 ± 1.89	0.098 ± 0.31

The cut flow on signal and background events after requiring the parton level cuts $\not{E}_T > 100$ GeV and $p_T(j_1) > 120$ GeV for $M_{Z'} \simeq 2448$ GeV and $g_{B-L} = 0.4$ at $\sqrt{s} = 14$ TeV with $\mathcal{L}dt = 300$ fb^{-1}:
(1) n(jets) ≥ 1 with $|\eta(j_1)| < 2$; (2) $p_T(j_1) > 500$ GeV; (3) $\not{E}_T > 500$ GeV;
(4) $\Delta\phi(j_2, \not{E}_T) > 0.5$; (5) veto on $p_T(j_2) > 100$ GeV, $|\eta(j_2)| < 2$;
(6) veto on $p_T(j_3) > 30$ GeV, $|\eta(j_3)| < 4.5$; (7) veto on e;
(8) veto on μ; (9) veto on τ-jets; (10) veto on b-jets.

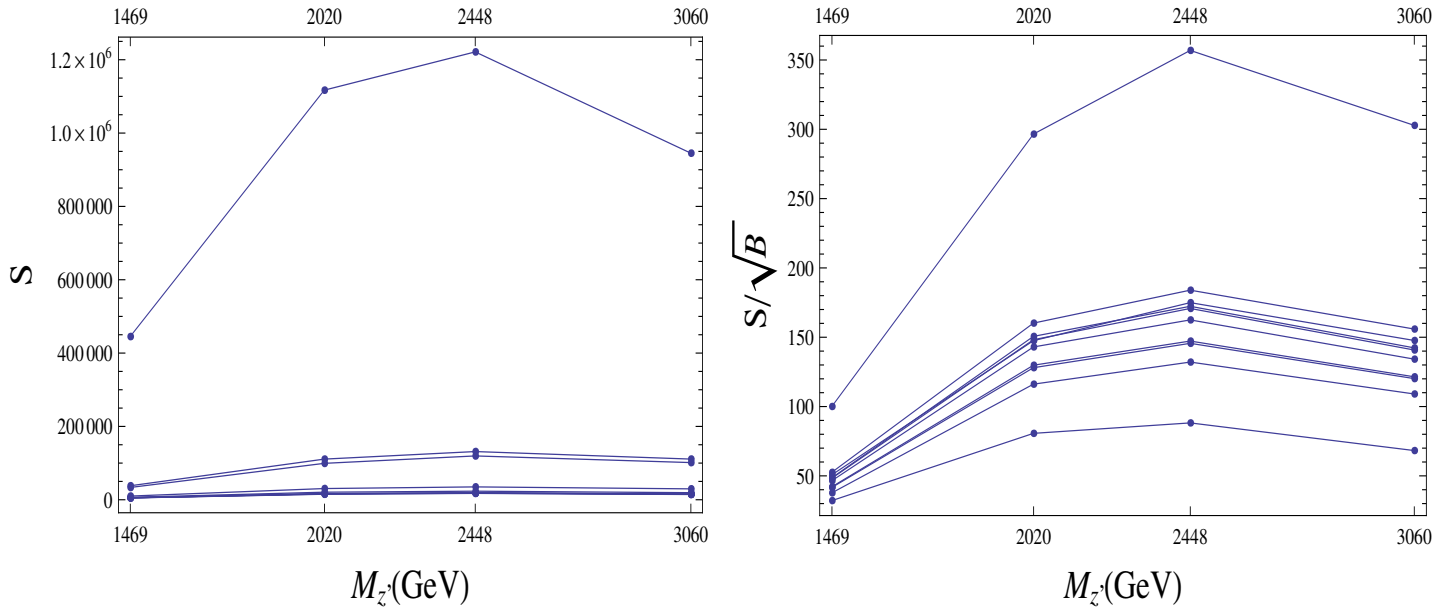

Number of events from the sum of all signals (S) versus $M_{Z'}$ and number of events from the sum of all signals divided by the square root of the total background ($S/\sqrt{B}$) versus $M_{Z'}$. Rates are given at 14 TeV for an integrated luminosity of 300 fb^{-1}.

Outline

1 Motivation

2 Analysis and Simulation

3 Summary

4 References

- We have shown that the LHC run 2 with standard luminosity can probe invisible signals which emerge in the BLSSM from Z' decays.

- We have shown that the LHC run 2 with standard luminosity can probe invisible signals which emerge in the BLSSM from Z' decays.
- We were able, by BLSSM specific cuts, to establish signals with significances well above 5σ discovery limit. Indeed, this has been possible due to the fact that the BLSSM mediator of such invisible signals is a very heavy Z', thereby transferring to its decay products large transverse momenta that can be generically exploited in all cases for background reduction.

- We have shown that the LHC run 2 with standard luminosity can probe invisible signals which emerge in the BLSSM from Z' decays.
- We were able, by BLSSM specific cuts, to establish signals with significances well above 5σ discovery limit. Indeed, this has been possible due to the fact that the BLSSM mediator of such invisible signals is a very heavy Z', thereby transferring to its decay products large transverse momenta that can be generically exploited in all cases for background reduction.
- For all topologies considered, the dominant component of the signal is via RH sneutrinos (above neutrinos and neutralinos), this fact help in distinguishing the BLSSM model from the popular SUSY models.

Outline

1 Motivation

2 Analysis and Simulation

3 Summary

4 References

1. W. Abdallah, J. Fiaschi, S. Khalil and S. Moretti, arXiv:1510.06475 [hep-ph].
2. S. Khalil, J. Phys. G **35**, 055001 (2008);
3. A. Elsayed, S. Khalil, S. Moretti and A. Moursy, Phys. Rev. D **87**, 053010 (2013).
4. M. Drees, M. Hanussek and J. S. Kim, Phys. Rev. D **86**, 035024 (2012).
5. N. F. Bell, J. B. Dent, A. J. Galea, T. D. Jacques, L. M. Krauss and T. J. Weiler, Phys. Rev. D **86**, 096011 (2012).
6. CMS Collaboration, CMS-EXO-12-061, arXiv:1412.6302 [hep-ex].

Thank you